General and Comparative Endocrinology 281 (2019) 49–57

Contents lists available at ScienceDirect

General and Comparative Endocrinology

journal homepage: www.elsevier.com/locate/ygcen

Molecular cloning of two *kcnk3* genes from the Northern snakehead (*Channa argus*) for quantification of their transcriptions in response to fasting and refeeding

Zheng-Yong Wen[a,c,d], Jun Wang[d], Chao Bian[b], Xinhui Zhang[b], Jia Li[b], Yuxiang Peng[a], Qiuyao Zhan[a], Qiong Shi[a,b,*], Yuan-You Li[c,*]

[a] BGI Education Center, University of Chinese Academy of Sciences, Shenzhen 518083, China
[b] Shenzhen Key Lab of Marine Genomics, Guangdong Provincial Key Lab of Molecular Breeding in Marine Economic Animals, BGI Academy of Marine Sciences, BGI Marine, BGI, Shenzhen 518083, China
[c] School of Marine Sciences, South China Agricultural University, Guangzhou 510642, China
[d] College of Life Sciences, Conservation and Utilization of Fishes Resources in the Upper Reaches of the Yangtze River Key Laboratory of Sichuan Province, Neijiang Normal University, Neijiang 641100, China

ARTICLE INFO

Keywords:
kcnk3
Phylogenetic analysis
Tissue distribution
Fasting
Refeeding
Northern snakehead (*Channa argus*)

ABSTRACT

Potassium channel subfamily K member 3 (KCNK3) has been reported to play important roles in membrane potential conduction, pulmonary hypertension and thermogenesis regulation in mammals. However, its roles remain largely unknown and scarce reports were seen in fish. In the present study, we for the first time identified two *kcnk3* genes (*kcnk3a* and *kcnk3b*) from the carnivorous Northern snakehead (*Channa argus*) by molecular cloning and a genomic survey. Subsequently, their transcription changes in response to different feeding status were investigated. Full-length coding sequences of the *kcnk3a* and *kcnk3b* genes are 1203 and 1176 bp, encoding 400 and 391 amino acids, respectively. Multiple alignments, 3D-structure prediction and phylogenetic analysis further suggested that these *kcnk3* genes may be highly conserved in vertebrates. Tissue distribution analysis by real-time PCR demonstrated that both the snakehead *kcnk3s* were widely transcribed in majority of the examined tissues but with different distribution patterns. In a short-term (24-h) fasting experiment, we observed that brain *kcnk3a* and *kcnk3b* genes showed totally opposite transcription patterns. In a long-term (2-week) fasting and refeeding experiment, we also observed differential change patterns for the brain *kcnk3* genes. In summary, our findings suggest that the two *kcnk3* genes are close while present different transcription responses to fasting and refeeding. They therefore can be potentially selected as novel target genes for improvement of production and quality of this economically important fish.

1. Introduction

Two-pore-domain potassium channels (K2P) underlie leakage of K^+ currents and are mainly distributed throughout the central nervous system, with supposed involvements in resting membrane potential of neurons and regulating their excitability (Aller et al., 2005; Mathie, 2007). In mammals, 15 members of the K2P family were identified, and they were divided into six subfamilies based on their structural and functional properties, including TASK (TASK1, TASK3, TASK5), TWIK (TWIK1, TWIK2, KCNK7), TALK (TALK1, TALK2, TASK2), TREK (TREK1, TREK2, TRAAK), THIK (THIK1, THIK2) and TRESK (Goldstein et al., 2001; Lesage, 2003).

The first cloned TASK channel gene, *TASK1*, also named as *KCNK3* (potassium channel subfamily K member 3), has been established as a site that can be modulated by a variety of agents, such as unsaturated fatty acids, extracellular pH, hypoxia, anaesthetics and intracellular signalling pathways (Olschewski et al., 2017; Talley and Bayliss, 2002). This modulation appears to be important in several physiological processes, including regulation of breathing (Cotten, 2013), control of aldosterone secretion (Czirjak et al., 2000), and transmitter and anesthetic regulation of neuronal activity (Davies et al., 2008). In addition, many studies revealed that mutants of KCNK3 were functionally related to both familial and idiopathic pulmonary arterial hypertension (Olschewski et al., 2017; Roberts, 2013). Recently, a genome-wide association study (GWAS) reveled that human KCNK3 was associated with obesity and food intake (Abou Ziki and Mani, 2016), which

* Corresponding authors at: BGI Education Center, University of Chinese Academy of Sciences, Shenzhen 518083, China.
E-mail addresses: shiqiong@genomics.cn (Q. Shi), yyli16@scau.edu.cn (Y.-Y. Li).

https://doi.org/10.1016/j.ygcen.2019.05.016
Received 15 March 2019; Received in revised form 6 May 2019; Accepted 18 May 2019
Available online 20 May 2019

suggested KCNK3 might be involved in energy balance and appetite regulation. However, these potential mechanisms still need to be further investigated.

Recent transcriptome studies revealed that the *Kcnk3* gene is transcribed not only in nervous systems but also in brown and beige adipose tissues of mice and humans (Feliciangeli et al., 2015; Pisani et al., 2016), and further experiments suggested that the KCNK3 protein acts as a positive regulator of thermogenesis through the mineralocorticoid receptor pathway (Pisani et al., 2016). However, another study reported that the *Kcnk3* transcription in thermogenic adipocytes was directly regulated by Prdm16 (PR domain containing 16; a transcription coregulator), and *Kcnk3* negatively regulated thermogenesis by dampening cAMP-PKA signaling (Chen et al., 2017). More experiments indicated that *Kcnk3* gene mediated outward K^+ current to antagonize depolarization induced Ca^{2+} influx, and the adipose-specific *Kcnk3*-knockout mice are resistant to hypothermia and obesity (Chen et al., 2017). It seems that the *Kcnk3* gene may be also involved in energy balance and lipid metabolism, which could be developed as a functional locus for improvement of lipid utilization in other animals including aquaculture fishes.

In fish, to our knowledge, rare publication focused on the *kcnk3* gene. However, we found some clues in big datasets from several fish transcriptome papers. For instance, the *kcnk3* was up-regulated in the brain of female medaka in response to hypoxia but not in male (Lai et al., 2016), and it had higher transcription levels in the gill of tilapia cultured in freshwater than in seawater (Lam et al., 2014). These studies suggested that fish *kcnk3* may be involved in hypoxia adaptation and ion-osmoregulation.

In order to improve the practical applications of this functional gene (such as development of high-quality fish varieties), we attempt to identify two homologues of mammalian *Kcnk3* gene from an economically important fish, Northern snakehead (*Channa argus*), and then we performed a series of bioinformatics analyses on these identified *kcnk3* genes. Subsequently, we detected their tissue distribution patterns and examined their transcription changes in the snakehead in response to different feeding status. To our knowledge, this is the first comprehensive report of *kcnk3* genes in a specific teleost. Our results will provide novel insights into functional roles (especially in energy balance) for practical applications of fish KCNK3s.

2. Materials and methods

2.1. Fish sampling

Obtained from the local Neijiang Fish Farm, juvenile Northern snakehead (*C. argus*; average weight of 71.3 ± 5.6 g) were transported to Neijiang Normal University (Neijiang, China) for fasting and refeeding experiments. Fishes were kept in 100-L (60 cm × 40 cm × 40 cm) tanks under natural light–dark conditions (12 L/12 D) with a constant flow of filtered water (18–20 °C). They were fed with commercial fish meat (5–8% of body weight) once a day at 19:00.

After acclimation for 2 weeks, six fishes were randomly selected for molecular cloning and tissue distribution studies. Fishes were anesthetized on ice before sacrificing by decapitation. Eleven tissue samples including adipose, brain, eye, gill, heart, intestine, kidney, liver, muscle, gonad (ovary) and spleen, were collected from each fish and immediately frozen in liquid nitrogen until use.

For the short-term food deprivation experiment, fishes were sampled with collection of brains (five from each group) at 19:15 (fishes were fed at 19:00 and allowed 15 min for eating, 0 h), 22:15 (3 h), 01:15 (6 h), 07:15 (12 h) and 19:15 (24 h) after feeding. For the long-term food deprivation and refeeding experiment, fishes were assigned to three experimental tanks (20 individuals per tank; 1 tank for feeding at 19:00 every day as controls and 2 tanks for fasting) for 2 weeks. The control group and one fasting with refeeding group were fed at 19:00 and sampled at 19:15, while the fishes in another fasting group were still fasted (the fasting group) and also sampled at 19:15. Subsequently, five fishes from each tank were randomly selected and brains were collected. All samples were kept at −80 °C until use.

All the animal experiments were conducted in accordance with the Chinese Ministry of Science and Technology for Humane Treatment of Laboratory Animals, and approved by the Animal Care and Use Committee of Neijiang Normal University.

2.2. Molecular cloning of two kcnk3 genes from C. Argus

Total RNA was isolated from each brain with the Trizol reagent (Invitrogen, Carlsbad, CA, USA) according to manufacturer's protocol, and 1 μg of the extracted RNA was reversely transcribed to cDNA using Super Script™ II RT reverse transcriptase (Thermo Fisher Scientific, Shanghai, China). Based on the genomic DNA sequences identified from our genome database and cDNA sequences from our transcriptome database (Xu et al., 2017), we designed four pairs of primers (see details in Supplementary Table 1) to amplify the full-length cDNA sequences of snakehead *kcnk3a* and *kcnk3b* genes. The basic cycling conditions of the PCRs were set as follows: a denaturing stage at 94 °C for 30 s, gene-specific annealing for 45 s and elongation stage at 72 °C for 60 s, a total of 35 cycles. The target products were purified from agarose gel using the Universal DNA Purification Kit (Tiangen, Beijing, China), and then cloned into a pMD-19 T vector (TaKaRa, Dalian, China). The final cDNA fragments were sequenced at BGI-Wuhan (Wuhan, China).

2.3. Sequence analysis and data processing

Each coding sequence (CDS) was identified by using the online software ORF finder (https://www.ncbi.nlm.nih.gov/gorf/gorf.html), and then the putative protein sequence was translated with Primer Premier 5.0 (Primer Biosoft International, Palo Alto, CA, USA). Moreover, the public Bioedit software was used to determine the isoelectric point (PI), and to perform multiple sequence alignments as described in our previous works (Wen et al., 2017; Yang et al., 2018). Furthermore, prediction of 3D-structure models of the selected KCNK3s were performed using the online tool SWISS-MODEL (https://www.swissmodel.expasy.org/interactive). Finally, synteny and gene structures of two fish *kcnk3* genes were compared on the basis of a comparative genomic survey, and the zebrafish genome assembly (GRCz11, Ensembl) was used as the reference to collect tutorial information.

2.4. Phylogenetic analysis

The deduced KCNK3 protein sequences of Northern snakehead and the KCNK3 protein sequences of several teleost species (see details in Fig. 3; downloaded from the NCBI) were aligned by CLUSTAL X2.1 (http://www.clustal.org/clustal2/). The aligned amino acid data sets were used to reconstruct a phylogenetic tree with the maximum likelihood (ML) approach using Mega 6.0 software (Li et al., 2019; Zou et al., 2017). The best-fitting model was calculated by Mrmodeltest 2.0 (Nylander, 2004) and ProtTest 2.4 (Abascal et al., 2005), and the JTT + G model was selected as the best. Robustness of the tree topology was assessed by a nonparametric bootstrap analysis with 1,000 resampling replicates. Moreover, for the phylogenetic tree, spotted gar was used as the outgroup. All the corresponding protein sequences were provided in Fig. 3.

2.5. Quantification by real-time PCR

Extraction of total RNA from fish tissues and first strand cDNA synthesis were performed as described above. Real-time PCR was conducted to detect mRNA levels of the snakehead brain *kcnk3*s with a Light Cycler Real-Time system (Roche Molecular Systems Inc., Pleasanton, CA, USA). Reversely transcribed products were used for the

real-time PCR in a final volume of 10 μL. Final products of the PCRs were verified with the melting curves that showed a single peak specific for the target genes. Relative transcription levels were calculated (Qin et al., 2018; Wen et al., 2015), and *tubα1* was used as the representative reference gene because of its high stability (although β-*actin* and other three more genes were also examined with good results; data not shown). Quantification primers for amplification of the snakehead *kcnk3a*, *kcnk3b* and *tubα1* were listed in Supplementary Table 1 (the last 3 pairs).

2.6. Statistical analysis

Statistical analysis was performed with SPSS 19.0 (IBM, Armonk, NY, USA). Significant differences were determined using one-way analysis of variance (ANOVA), followed by the post hoc test (least significant difference test and Duncan's multiple range test), after confirming data normality and homogeneity of variances. All data were expressed as the mean ± SEM (standard error of the mean). Differences were considered to be significant when $P < 0.05$.

3. Results

3.1. Molecular identification of two snakehead kcnk3 genes

Two specific PCR fragments were obtained and sequenced for the snakehead *kcnk3a* and *kcnk3b* genes, respectively. Subsequently, both were assembled into individual complete gene sequence based on our previous genome report (Xu et al., 2017). The final nucleotide fragments of the snakehead *kcnk3a* and *kcnk3b* were 1,607 and 1,721 bp in length (GenBank accession nos. MK559417 and MK214759; see more details in Figs. 1 and 2 respectively).

For the snakehead *kcnk3a* sequence (Fig. 1), it contains a 232-bp 5′-UTR, a 173-bp 3′-UTR, and a 1,203-bp open reading frame (ORF) encoding 400 putative amino acid residues. Similarly, the snakehead *kcnk3b* sequence (Fig. 2) includes a 207-bp 5′-UTR, a 337-bp 3′-UTR, and a 1,176-bp ORF encoding 391 putative amino acid residues. Both deduced protein sequences (Figs. 1, 2) had six transmembrane α-helix domains, which were highly conserved among vertebrates including fishes. Moreover, a predicted N-linked glycosylation site and a phosphorylation site were localized in the N-terminal and the C-terminal of the two genes (green and blue oval boxes in Figs. 1 and 2), respectively.

3.2. Multiple alignments and predicted three-dimensional structures of the snakehead KCNK3s

Aligning of multiple amino acid sequences could be helpful for better understanding of structural and functional properties of the examined proteins. Here, we observed that KCNK3s are highly conserved across the vertebrates, sharing similar structural characteristics (such as six conserved transmembrane α-helix domains, a N-terminal linked glycosylation site and a C-terminal linked phosphorylation site; see Fig. 3A). It is notable that the peptide sequences from the position 270 to 390 are variable and nonconservative (Fig. 3), and the KCNK3a is approximately 11 residues longer than its paralog KCNK3b at the position 280–300 (Fig. 3A).

In addition, sequence comparisons showed that the snakehead KCNK3a shared 49.2 ~ 68.7% identity with its counterparts from human (68.7%), mouse (66.1%), chicken (70.6%), lizard (54.8%) and frog (49.2%), respectively, and it shared a higher identity with its homologs from teleost species (tilapia: 91%, fugu: 89.7%, medaka: 82.2% and zebrafish: 73.9%; see more details in Supplemental Table 2). However, the snakehead KCNK3b showed a lower identity with its counterparts from vertebrates, such as 62.7%, 60.3%, 65.6%, 47%, and 50.8% identity with those from human, mouse, chicken, lizard and frog respectively; while it still shared a higher identity with its homologs from fish species (such as tilapia: 88.7%, fugu: 87.4%, medaka: 82.8% and zebrafish: 69.6; see Supplemental Table 2).

Moreover, both the snakehead KCNK3s are significantly different

```
-232                                                gtttccctgggctggaaagcgagggaaggatagatgggtggaggaggaggat  -181
-180  tcctgtagtgggaggtgaggtagggaggggtggtgctgaatgaacagctcctctgctcattaagtaatcagagagctcctctgctccgtc   -91
-90   agagcagcacagccatgaaccaaccgagctccccgtcctccagaccagcgccgacactccgcctgtccccctgacacacgccgcaccacc    -1
1     ATGAAGAGGCAAAACGTGAGGACGCTCGCCCTCATCATATGCACCTTCACCTACCTGATCGTCGGCGCGGCGATCTTCGACGCGCTGGAA    90
1      M  K  R  Q  N  V  R  T  L  A  L  I  I  C  T  F  T  Y  L  I  V  G  A  A  I  F  D  A  L  E    30
91    TCCCGACAGGAGACGAACCAGAGGAAAGAGCTGGACCAGAGGAAAGCGGAGCTGCTCAAGACGTTCAACTTGTCCAGGGAGGACTTTGAC   180
31     S  R  Q  E  T  N  Q  R  K  E  L  D  Q  R  K  A  E  L  L  K  T  F  N  L  S  R  E  D  F  D    60
181   GAGCTGGAGAAGGTGGTGCTGCAGCTGAAGCCGCACAAAGCCGGGGTGCAGTGGAAATTCGCAGGCTCGTTTTACTTCGCCATCTCTGTG   270
61     E  L  E  K  V  V  L  Q  L  K  P  H  K  A  G  V  Q  W  K  F  A  G  S  F  Y  F  A  I  S  V    90
271   ATCACGACCATAGGGTATGGCCACGCAGCCCCCAGCACAGATGTGGGGAAGGTGTTCTGCATGCTCTACGCCCTCCTGGGCATCCCTCTC   360
91     I  T  T  I  G  Y  G  H  A  A  P  S  T  D  V  G  K  V  F  C  M  L  Y  A  L  L  G  I  P  L   120
361   ACTTTGGTCATGTTCCAGAGTGTCGGTGAGCGGATCAACACCTTTGTCAGGTACCTGCTTCACCGCCTGAAGAAGTGCCTTGGCATGAGG   450
121    T  L  V  M  F  Q  S  V  G  E  R  I  N  T  F  V  R  Y  L  L  H  R  L  K  K  C  L  G  M  R   150
451   CGCACTGAGGTCTCCATGGTCAACATGGTGACCATTGGTTTCATATCTTGCATGAGCACATTGTGTGTGGGGGCACTGGCCTTCTCCCAC   540
151    R  T  E  V  S  M  V  N  M  V  T  I  G  F  I  S  C  M  S  T  L  C  V  G  A  L  A  F  S  H   180
541   TTTGAGGGATGGAGTTTCTTTCATGCCTACTACTACTGCTTCATCACGCTCACCACCATTGGCTTCGGGGACTATGTGGCACTGCAGAAT   630
181    F  E  G  W  S  F  F  H  A  Y  Y  Y  C  F  I  T  L  T  T  I  G  F  G  D  Y  V  A  L  Q  N   210
631   GAGCATGCACTGCAGAACAAGCCAGAATATGTGGCCTTCTGCTTCATCTACATCCTGACCGGTCTGGCTGTGATTGGAGCCTTCCTCAAC   720
211    E  H  A  L  Q  N  K  P  E  Y  V  A  F  C  F  I  Y  I  L  T  G  L  A  V  I  G  A  F  L  N   240
721   TTAGCAGTGCTGCGCTTCATGACCATGAACACTGAGGACGAGAAGAGGGATGCAGAGCAGAGGGCGCTCCTCGCTCATAACGGTCAGGTG   810
241    L  A  V  L  R  F  M  T  M  N  T  E  D  E  K  R  D  A  E  Q  R  A  L  L  A  H  N  G  Q  V   270
811   GGAGGACACATCCACTGCTCTGTAGACCTCCCTTCATCCCCCTCCACGCCCACTGGCTGTGGCGGAGGAAGCACAGCCGGAGGAGGCGGC   900
271    G  G  H  I  H  C  S  V  D  L  P  S  S  P  S  T  P  T  G  C  G  G  G  S  T  A  G  G  G  G   300
901   GGAGGAGCAGCGAGCCGAGGTTTACGTAACGTTTACGCAGAGGTACTCCACTTCCAGTCCATGTGCTCCTGCCTTTGGTACAAGAGTAGA   990
301    G  G  A  A  S  R  G  L  R  N  V  Y  A  E  V  L  H  F  Q  S  M  C  S  C  L  W  Y  K  S  R   330
991   GAGAAGCTGCAATACTCTATACCCATGATCATCCCCTGTGACCTCTCCACCTCGGACACCTACATGGAGCAAGGAGAGGCTTTTTCCAAC  1080
331    E  K  L  Q  Y  S  I  P  M  I  I  P  C  D  L  S  T  S  D  T  Y  M  E  Q  G  E  A  F  S  N   360
1081  CCCCTCCACTCTAATGGCTGCGTGTGCAGCCTGCAGCGTCACTCTGGCATCAGCTCGGTGTCCACTGGTCTGCAGAGCATCAACACCTAC  1170
361    P  L  H  S  N  G  C  V  C  S  L  Q  R  H  S  G  I  S  S  V  S  T  G  L  Q  S  I  N  T  Y   390
1171  AGAAGACTCAATAAACGCAGAAGCTCCATCTAAaccaggcgaacatcacgctttaaggtcaagttgtacttttgtccaccatgtggtgag  1203
391    R  R  L  N  K  R  R  S  S  I  *                                                            400
1261  gatgggccctcatgatgtggtactacatcagagagacaaaaactccggtcttaataagacacagtacttctgatgtttgcttctctctga  1350
1351  Cactgaggagtctctacagtctttt                                                                  1376
```

Fig. 1. Complete cDNA and deduced protein sequences of the snakehead *kcnk3a* gene. Putative transmembrane conserved domains are labeled in boxes. Small letters in the top and bottom areas represent the 5′- and 3′-untranslated regions (UTRs). The predicted N-linked glycosylation site and phosphorylation site are emphasized in the green and blue oval boxes, respectively. Underlines represent the initiation codon and termination codon respectively. The stop codon is marked by an asterisk (*).

Fig. 2. Complete cDNA and deduced protein sequences of the snakehead *kcnk3b* gene. Putative transmembrane conserved domains are labeled in boxes. Small letters in the top and bottom areas represent the 5′- and 3′-untranslated regions (UTRs). The predicted N-linked glycosylation site and phosphorylation site are emphasized in the green and blue oval boxes, respectively. Underlines represent the initiation codon and termination codon respectively. The stop codon is marked by an asterisk (*).

from each other, since the KCNK3a shared only 64.3% identity with KCNK3b (Supplemental Table 2). A three-dimensional (3D) structure analysis demonstrated that the snakehead KCNK3b but not KCNK3a was quite similar to human, mouse and chicken counterparts (only one in each non-fish vertebrate), and it is significantly different from the snakehead KCNK3a (Fig. 3B). The electronic point and molecular weights of the snakehead KCNK3a and KCNK3b were calculated to be 8.50 & 9.07 and 44.44 & 44.01 KD, respectively.

3.3. Comparative analysis of kcnk3a and kcnk3b in zebrafish and snakehead genomes

Thus far, only a single copy of *kcnk3* gene was determined in tetrapods while our data showed that two *kcnk3* genes are widely existed in fish species (Fig. 3). In order to verify the widespread existence of both *kcnk3* genes in teleost, representative genomic synteny and gene structures of zebrafish and snakehead *kcnk3*s were presented (Fig. 4). We observed that the zebrafish *kcnk3a* and *kcnk3b* are differentially localized. The former is located in the chromosome 20, and it is surrounded by *pp2r5a* and *enpp1* genes; while the latter is located in chromosome 17, and its location between *hhipl2* and *ezra* was confirmed (Fig. 4A). We also identified two *kcnk3* genes from the snakehead, and our genomic survey determined that the snakehead *kcnk3a* and *kcnk3b* genes are located on scaffolds 65 and 407, respectively. Interestingly, a 180° reversal of the snakehead genomic DNA fragment with four genes (including *kcnk3a*, *enpp1*, *sytl3* and *ezrb*) was identified in the scaffold 65, and thereby the snakehead *kcnk3a* gene is next to *enpp1* but not *ppp2r5a*, when compared with the corresponding fragment and genes of zebrafish (Fig. 4A). For the snakehead *kcnk3b*, however, we observed that it presented similar neighboring gene order with the zebrafish *kcnk3b*, as both were located between *hhipl2* and *ezra* (see Fig. 4A).

Gene structure analysis proved that both the zebrafish *kcnk3a* and *kcnk3b* genes consisted of two exons and one intron, which are the same as the snakehead *kcnk3*s (Fig. 4B). However, the introns of zebrafish and snakehead *kcnk3a* were 32.95 and 26.35 kb respectively, which are much longer than the corresponding introns of *kcnk3b* genes (approximately 2.67 and 2.42 kb respectively; Fig. 4B).

3.4. Phylogenetic analysis

For a better understanding of the evolutionary relationships among various vertebrate KCNK3s, we performed a phylogenetic analysis using the maximum likelihood (ML) method. The phylogenetic tree was reconstructed based on 22 KCNK3 protein sequences of various vertebrate species, ranging from fishes to mammals. It appears that, from the topology in Fig. 5, animals can be divided into two subgroups of tetrapods and fishes, and the fish subgroup can be further separated into two clades of *kcnk3a* and *kcnk3b* subtypes. Undoubtedly, the snakehead *kcnk3a* and *kcnk3b* were clustered into the teleost *kcnk3a* and *kcnk3b* clades, with a close relationship to tilapia *kcnk3a* and Amazon molly *kcnk3b*, respectively (see more details in Fig. 5).

3.5. Tissue distribution of the snakehead kcnk3s

Tissue distribution patterns of the two snakehead *kcnk3* genes were determined by quantitative real-time PCR. Eleven tissues were collected and detected. Our data demonstrated that the snakehead *kcnk3a* was widely transcribed in the examined tissues, especially in the heart and the brain (Fig. 6A). The transcription levels decreased as follows: heart > brain > intestine > spleen > kidney > adipose > gill > eye > muscle > ovary; whereas mRNA was not detectable in the liver. Similarly, the snakehead *kcnk3b* was also extensively distributed in the central and peripheral tissues (Fig. 6B). Unexpectedly, the snakehead *kcnk3b* was not detectable in the adipose tissue. In summary, the two *kcnk3* genes presented significantly differences in tissue

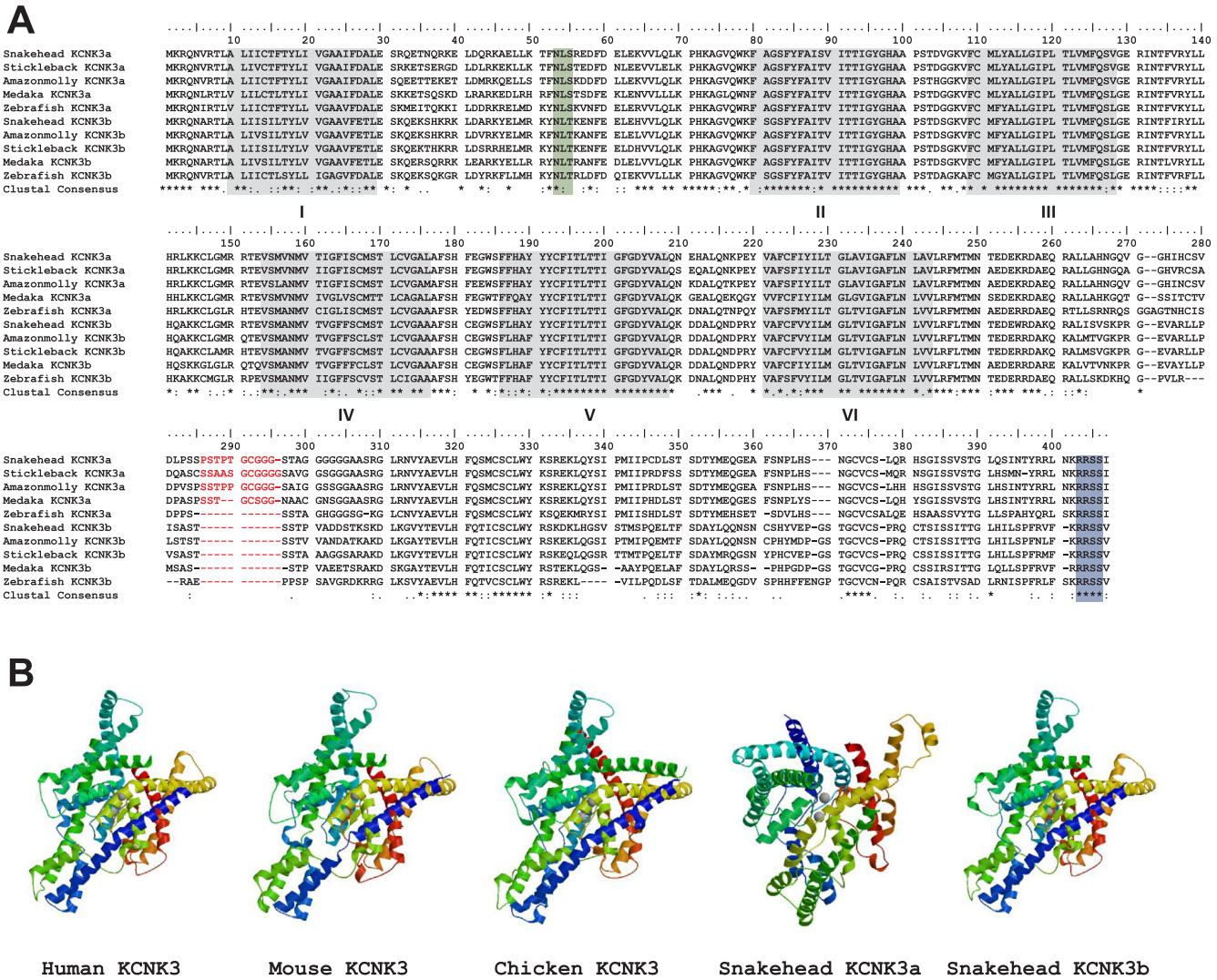

Fig. 3. Sequence alignment (**A**) and 3D-structural model comparisons (**B**) among the vertebrate KCNK3s. Dashes in the protein sequences represent gaps after the comparative alignment. Asterisks (*) indicate conservation of the amino acids among the examined sequences. Regions of the Six transmembrane α-helix domains are highlighted in grey and labeled with I to VI respectively. Predicted N-linked glycosylation site and phosphorylation site are marked in green and blue, respectively. Sequences and gaps in a red color represent a significant variation between KCNK3a and KCNK3b.

distribution pattern, although both were widely distributed in almost all the examined tissues.

3.6. Effects of food deprivation and refeeding on the transcriptions of both snakehead kcnk3 genes

To investigate transcription changes of the snakehead *kcnk3* genes in response to starvation and refeeding schemes, we measured the brain *kcnk3* mRNA levels during the short-term (24-h) and the long-term (2-week) food deprivation and refeeding experiments. For the short-term fasting experiment, we observed that the snakehead *kcnk3a* and *kcnk3b* genes showed totally opposite transcription patterns at 0, 3, 6, 12 and 24 h after fasting (see Fig. 7). Compared with the controls, the brain *kcnk3a* mRNA level was slightly increased at 3 h after fasting, then significantly elevated up to a 3-fold and a 2-fold values at 6 and 12 h after fasting, and finally fell down to the control level at 24 h after food deprivation (see more details in Fig. 7A). On the contrary, the brain *kcnk3b* mRNA level was slightly decreased at 3 h after fasting, then continuously decreased at 6 and 12 h after fasting, and at last elevated at 24 h after food deprivation to around 2-fold of the least value at 12 h after fasting (see Fig. 7B).

For the long-term fasting and refeeding experiment, we also observed different change patterns for the brain *kcnk3a* and *kcnk3b* transcriptions (Fig. 8). Compared to the control group, the *kcnk3a* mRNA levels were lower in both the fasted and the refed groups (Fig. 8A). However, the *kcnk3b* mRNA level was significantly increased to more than 4-fold after two weeks of food deprivation, and then it was dramatically decreased after an immediate refeeding to a level equivalent to the control (Fig. 8B).

4. Discussion

In the present study, two *kcnk3* genes (named *kcnk3a* and *kcnk3b*) were identified from the snakehead. The full-length coding sequence of the snakehead *kcnk3a* was 1,203 bp encoding a putative 400-aa protein, and the coding sequence of snakehead *kcnk3b* was 1,176 bp encoding a putative 391-aa protein. The snakehead *kcnk3b* is more similar to the human *KCNK3* than the snakehead *kcnk3a*, and further multiple sequence alignments suggested that fish KCNK3a is usually approximatively 10-aa longer than KCNK3b, although both seem to be widely existed in fish (Talley and Bayliss, 2002). Meanwhile, six transmembrane α-helix domains, a putative N-linked glycosylation site and a phosphorylation site were predicted in both snakehead KCNK3 protein sequences, which are highly conservative across vertebrates. However,

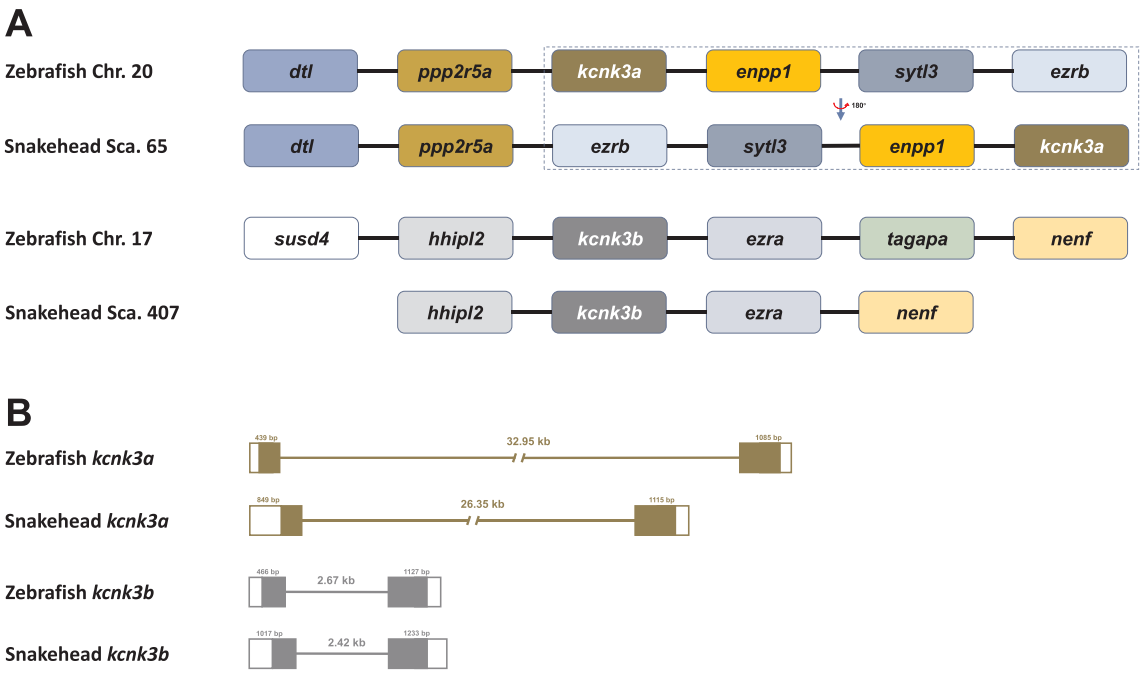

Fig. 4. Syntenic (**A**) and genomic (**B**) comparisons of the *kcnk3a* and *kcnk3b* genes in zebrafish and snakehead. The colorful blocks and solid lines represent genes and intergenic regions (in A), whereas stand for exons and introns (in B), respectively. As shown in the figure A, both *kcnk3* genes are identified in the two fish genomes, while a remarkable region is fragmental inverted between the two fish species. As shown in the figure B, numbers above the colorful boxes and lines represent the length of exons and introns, respectively.

the 3D structure of snakehead KCNK3a is significantly different from its paralog KCNK3b, suggesting that fish KCNK3 could possess different subtypes for various physiological functions.

In order to verify our previous hypothesis of potential applications, we analyzed the genomic synteny and gene structures of snakehead *kcnk3a* and *kcnk3b* using a genomic survey method, and then we compared these data with zebrafish *kcnk3a* and *kcnk3b*. These results showed that the snakehead *kcnk3a* is obvious different from the *kcnk3b*,

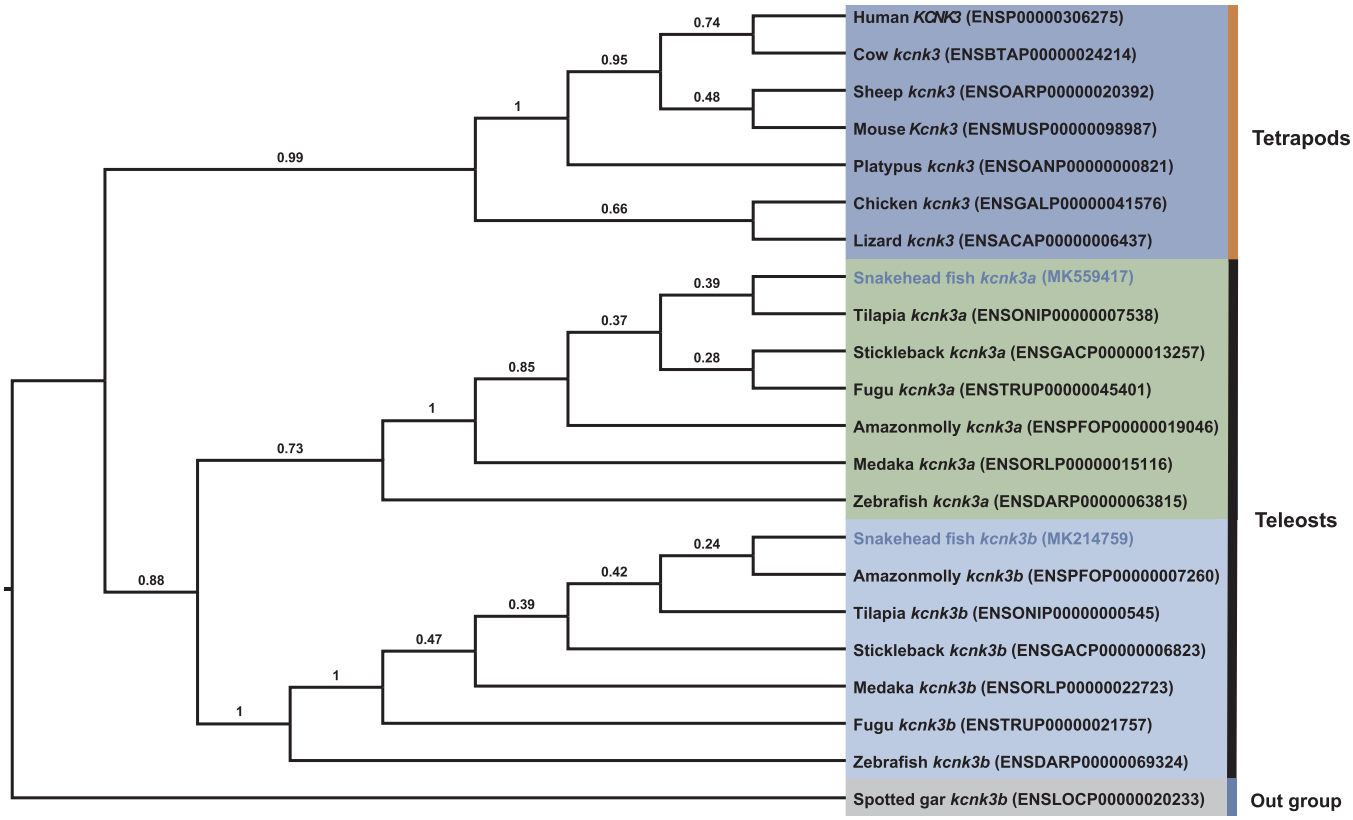

Fig. 5. A phylogenetic tree of vertebrate *kcnk3* genes. It was constructed based on 22 protein sequences using MEGA 6.0 program. Spotted gar *kcnk3b* was used as the outgroup. Values at the nodes represent bootstrap percentages from 1,000 replicates. Protein sequence IDs are provided in the brackets.

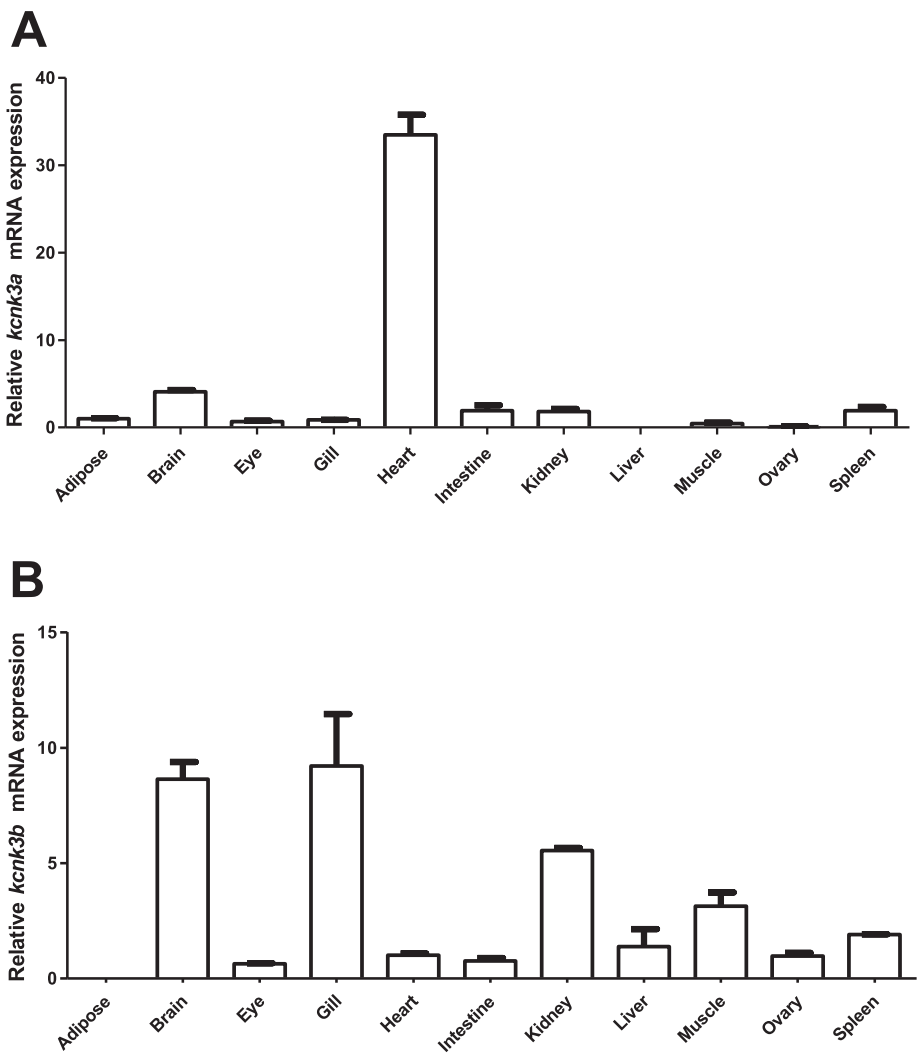

Fig. 6. Tissue distribution of the *kcnk3a* (**A**) and *kcnk3b* (**B**) genes in the Northern snakehead. Eleven tissues were detected in the present study. Results were expressed as relative expression levels and normalized by the *Tubα 1* gene. Each error bar represents a standard error of the mean (n = 6).

with localization at different genetic loci and exhibition of different gene orders and structures, which confirmed existence of two different *kcnk3* genes in the snakehead. This phenomenon might be generated by the teleost specific whole genome duplication event, which has been well known for occurrence in the process of fish evolution and also considered as an important driving force of biological evolution (Glasauer and Neuhauss, 2014; Jaillon et al., 2004; Meyer and Van de Peer, 2005). Furthermore, the genetic locus, gene sequence and structure, 3D protein structure of fish *kcnk3a* are significantly different from its paralog *kcnk3b*, suggesting their differential physiological roles in fish.

In order to investigate the evolutionary process of *kcnk3* in vertebrates, a phylogenetic tree was reconstructed based on a protein dataset of 22 sequences. We observed that vertebrates could be divided into two groups of tetrapod and teleost, and the teleost group can be further separated into two subgroups of *kcnk3a* and *kcnk3b* clades. The snakehead *kcnk3a* and *kcnk3b* were clustered into the fish clades of *kcnk3a* and *kcnk3b*, respectively. Interestingly, our data demonstrated that the snakehead *kcnk3a* is close to tilapia *kcnk3a*, whereas its paralog snakehead *kcnk3b* is more close to Amazon molly *kcnk3b*. It seems that fish *kcnk3a* and *kcnk3b* might have evolved independently and their potential roles need to be further investigated.

The tissue distribution patterns of snakehead *kcnk3a* and *kcnk3b* genes were determined using quantitative real-time PCR. We observed that *kcnk3a* was extensively transcribed both in the central and peripheral tissues, and with the most abundant levels in the heart and the brain (Fig. 6A). The highest transcriptions in the brain and the heart suggest its similar roles in resting membrane potential of neurons and regulating their excitability to those reported in mammals (Mathie, 2007; Talley and Bayliss, 2002). Surprisingly, the snakehead *kcnk3a* was not detected in the liver and very low in the adipose, which have been considered as important energy metabolism organs in fish (Qin et al., 2018). This distribution pattern is significantly different from the data in mammals, suggested that fish *kcnk3a* might be not participating in the regulation of thermogenesis.

Similarly, the snakehead *kcnk3b* also presented a wide distribution. The highest transcription in the brain indicated similar roles to its paralog *kcnk3a*. A high transcription of the snakehead *kcnk3b* in the gill (Fig. 6B) further suggests potential involvement in ion-osmoregulation and breathing regulation, which is consistent with a previous report of tilapia gill in response to different water salinity (Lam et al., 2014). Unexpected, the snakehead *kcnk3b* was very low in the liver and undetectable in the adipose tissue, which are remarkably different from the data in mammals (Feliciangeli et al., 2015; Pisani et al., 2016). Furthermore, relative high transcription levels in the spleen, muscle and heart suggest fish *kcnk3b* might mediate an acid-sensitive K^+-selective non-inactivating leak current to hyperpolarize the membrane and to decrease the excitability of cells as reported in mammals (Davies

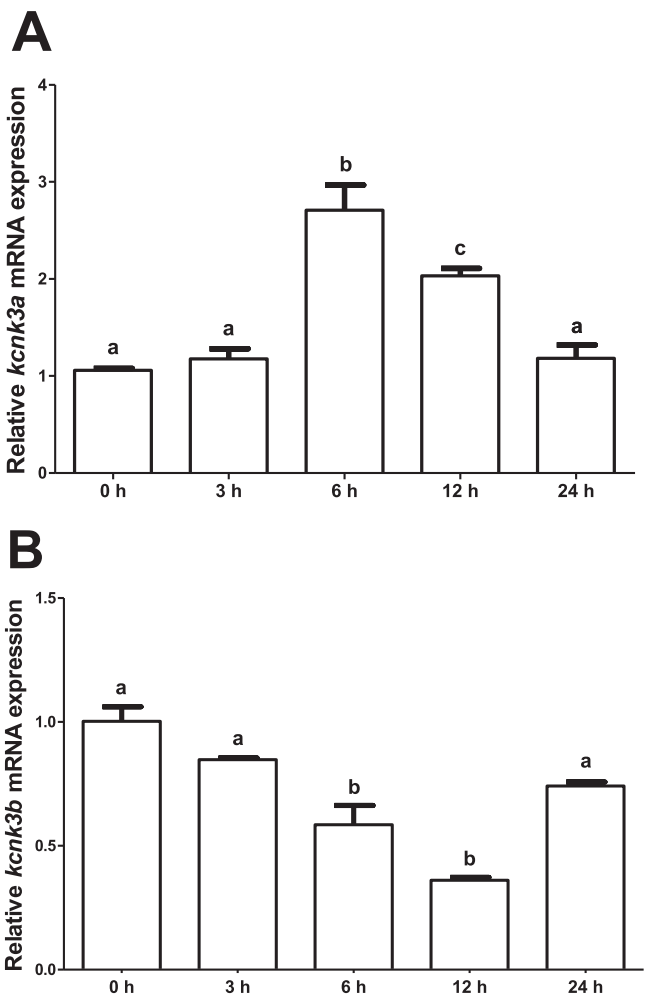

Fig. 7. Effects of a 24-h fasting on the transcriptions of *kcnk3a* (**A**) and *kcnk3b* (**B**) genes in the examined snakehead brains. *Tubα 1* was used to normalize gene transcriptions. Significant differences ($P < 0.05$) between groups were analyzed using a one-way ANOVA. Groups with significant differences are marked by different letters above the bars. Data are presented as mean ± SEM (n = 5).

et al., 2008; Feliciangeli et al., 2015).

As observed in Fig. 6, snakehead *kcnk3a* and *kcnk3b* exhibited different distribution patterns, suggested their differential physiological roles in different tissues. Snakehead *kcnk3a* should play more important roles in the heart and brain, while the snakehead *kcnk3b* could play more critical roles in the brain and gill. In addition, *kcnk3a* but not *kcnk3b* was detected in the adipose, suggesting that snakehead *kcnk3a* might play an important role in maintaining energy balance as found in mammals (Chen et al., 2017). Furthermore, *kcnk3b* but not *kcnk3a* was detected in the liver and ovary, implying that the *kcnk3b* might play important role in energy metabolism and ovary development. The different transcription patterns were also consistent with the structural and sequence differences of the snakehead KCNK3s.

In order to investigate whether KNCK3s play an important role in appetite regulation and energy balance or not, we detected the brain transcription changes in response to different feeding status. In the short-term (24-h) fasting experiment, the brain *kcnk3a* mRNA level was increased to the highest at 6 h after feeding, and then decreased to a low level (similar to the control) at 24 h after the food deprivation (Fig. 7A). This transcription pattern is similar to a previous report of neuropeptide Y (*npy*) gene in the snakehead brain after fasting (Yang et al., 2018), suggesting that *kcnk3a* might also serve as a short-term appetite regulator and an orexigenic factor in fish (Davies et al., 2008). In contrast to the *kcnk3a*, the snakehead brain *kcnk3b* was continuously decreased to the least level at 12 h after fasting, and then dramatically increased at 24 h after fasting (Fig. 7B). This finding was different from the snakehead *npy* transcription, but *kcnk3b* still presented significant changes as previously reported (Qin et al., 2018; Yang et al., 2018), suggesting that the snakehead *kcnk3b* might be a short-term appetite regulator with a potential anorexigenic effect in fish. The differential roles of these two genes might be a consequence of the fish specific whole genome duplication event (Glasauer and Neuhauss, 2014); however, the opposite transcription patterns suggest that the snakehead *kcnk3a* and *kcnk3b* might form a negative feedback during the physiological process of appetite regulation, although the exact reasons for the opposite effects are still a mystery.

In the long-term (2-week) fasting and refeeding experiment, the snakehead brain *kcnk3a* was slightly decreased both in the fasted and refed groups (Fig. 8A), suggesting that *kcnk3a* could not play as a long-term appetite regulator since a long-term fasting could reduce the activity of neurons to prevent energy consumption and hence to depress the transcription of the brain *kcnk3a*. On the contrary, snakehead *kcnk3b* was significantly increased after a two-weeks' continuous food deprivation, while it was subsequently dramatically decreased to a control level after an immediate refeeding (Fig. 8B). These findings are in line with the previous study of snakehead brain *npy* (Yang et al., 2018), suggesting that *kcnk3b* might serve as a long-term regulator of appetite and energy balance in the snakehead.

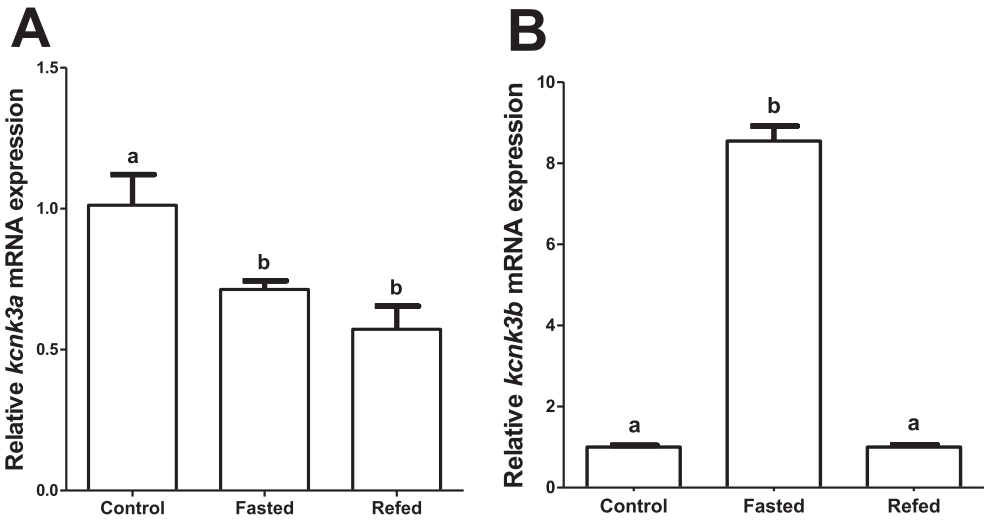

Fig. 8. Effects of a long-term (2-week) fasting and an immediate refeeding on the transcription of *kcnk3a* (**A**) and *kcnk3b* (**B**) genes in the examined snakehead brains. *Tubα 1* was used to normalize gene transcriptions. Significant differences ($P < 0.05$) between groups were analyzed using a one-way ANOVA. Groups with significant differences are marked by different letters above the bars. Data are presented as mean ± SEM (n = 5).

In conclusion, we identified both *kcnk3a* and *kcnk3b* genes from the Northern snakehead and functionally investigated its potential roles in response to different nutritional states for the first time. Our data confirm the ubiquitous subtypes of *kcnk3a* and *kcnk3b* in fish, and their conservation across vertebrates. Differential tissue distribution and transcription responses to fasting and refeeding, suggesting that the two *kcnk3* genes in snakehead fish might functional differently while co-operatively. Our present work provides new insights into the fish *kcnk3* genes (especially in energy balance) and suggest that they could be selected as important genetic loci for improving the production of this kind of fish.

Acknowledgments

This work was financially supported by Scientific Research Fund of Sichuan Education Department (no. 18ZB0328), Special Research Program of Neijiang Normal University (no. 17ZL03), and Shenzhen Special Program for Upgrading Key Links to Strategies for the Emerging and Future Industries (no. 20170428173357698).

Conflict of interest

The authors declare that they have no conflict of interest.

Appendix A. Supplementary data

Supplementary data to this article can be found online at https://doi.org/10.1016/j.ygcen.2019.05.016.

References

Abascal, F., Zardoya, R., Posada, D., 2005. ProtTest: selection of best-fit models of protein evolution. Bioinformatics 21, 2104–2105.
Abou Ziki, M.D., Mani, A., 2016. Metabolic syndrome: genetic insights into disease pathogenesis. Curr. Opin. Lipidol. 27, 162–171.
Aller, M.I., Veale, E.L., Linden, A.M., Sandu, C., Schwaninger, M., Evans, L.J., Korpi, E.R., Mathie, A., Wisden, W., Brickley, S.G., 2005. Modifying the subunit composition of TASK channels alters the modulation of a leak conductance in cerebellar granule neurons. J. Neurosci. 25, 11455–11467.
Chen, Y., Zeng, X., Huang, X., Serag, S., Woolf, C.J., Spiegelman, B.M., 2017. Crosstalk between KCNK3-Mediated Ion Current and Adrenergic Signaling Regulates Adipose Thermogenesis and Obesity. Cell 171, 836–848.
Cotten, J.F., 2013. TASK-1 (KCNK3) and TASK-3 (KCNK9) tandem pore potassium channel antagonists stimulate breathing in isoflurane-anesthetized rats. Anesth. Analg. 116, 810–816.
Czirjak, G., Fischer, T., Spat, A., Lesage, F., Enyedi, P., 2000. TASK (TWIK-related acid-sensitive K+ channel) is expressed in glomerulosa cells of rat adrenal cortex and inhibited by angiotensin II. Mol. Endocrinol. 14, 863–874.
Davies, L.A., Hu, C., Guagliardo, N.A., Sen, N., Chen, X., Talley, E.M., Carey, R.M., Bayliss, D.A., Barrett, P.Q., 2008. TASK channel deletion in mice causes primary hyperaldosteronism. Proc. Natl. Acad. Sci. USA 105, 2203–2208.
Feliciangeli, S., Chatelain, F.C., Bichet, D., Lesage, F., 2015. The family of K2P channels: salient structural and functional properties. J. Physiol. 593, 2587–2603.
Glasauer, S.M., Neuhauss, S.C., 2014. Whole-genome duplication in teleost fishes and its evolutionary consequences. Mol. Genet. Genomics 289, 1045–1060.
Goldstein, S.A., Bockenhauer, D., O'Kelly, I., Zilberberg, N., 2001. Potassium leak channels and the KCNK family of two-P-domain subunits. Nat. Rev. Neurosci. 2, 175–184.
Jaillon, O., Aury, J.M., Brunet, F., Petit, J.L., Stange-Thomann, N., Mauceli, E., Bouneau, L., Fischer, C., Ozouf-Costaz, C., Bernot, A., Nicaud, S., Jaffe, D., Fisher, S., Lutfalla, G., Dossat, C., Segurens, B., Dasilva, C., Salanoubat, M., Levy, M., Boudet, N., Castellano, S., Anthouard, V., Jubin, C., Castelli, V., Katinka, M., Vacherie, B., Biemont, C., Skalli, Z., Cattolico, L., Poulain, J., De Berardinis, V., Cruaud, C., Duprat, S., Brottier, P., Coutanceau, J.P., Gouzy, J., Parra, G., Lardier, G., Chapple, C., McKernan, K.J., McEwan, P., Bosak, S., Kellis, M., Volff, J.N., Guigo, R., Zody, M.C., Mesirov, J., Lindblad-Toh, K., Birren, B., Nusbaum, C., Kahn, D., Robinson-Rechavi, M., Laudet, V., Schachter, V., Quetier, F., Saurin, W., Scarpelli, C., Wincker, P., Lander, E.S., Weissenbach, J., Roest Crollius, H., 2004. Genome duplication in the teleost fish Tetraodon nigroviridis reveals the early vertebrate proto-karyotype. Nature 431, 946–957.
Lai, K.P., Li, J.W., Tse, A.C., Wang, S.Y., Chan, T.F., Wu, R.S., 2016. Differential responses of female and male brains to hypoxia in the marine medaka *Oryzias melastigma*. Aquat. Toxicol. 172, 36–43.
Lam, S.H., Lui, E.Y., Li, Z., Cai, S., Sung, W.K., Mathavan, S., Lam, T.J., Ip, Y.K., 2014. Differential transcriptomic analyses revealed genes and signaling pathways involved in iono-osmoregulation and cellular remodeling in the gills of euryhaline Mozambique tilapia, *Oreochromis mossambicus*. BMC Genomics 15, 921.
Lesage, F., 2003. Pharmacology of neuronal background potassium channels. Neuropharmacology 44, 1–7.
Li, R., Wang, G., Wen, Z.Y., Zou, Y.C., Qin, C.J., Luo, Y., Wang, J., Chen, G.H., 2019. Complete mitochondrial genome of a kind of snakehead fish *Channa siamensis* and its phylogenetic consideration. Genes & Genomics 41, 147–157.
Mathie, A., 2007. Neuronal two-pore-domain potassium channels and their regulation by G protein-coupled receptors. J. Physiol. 578, 377–385.
Meyer, A., Van de Peer, Y., 2005. From 2R to 3R: evidence for a fish-specific genome duplication (FSGD). Bioessays 27, 937–945.
Nylander, J.A.A., 2004. MrModeltest v2. Program Distributed by the Author. Evolutionary Biology Centre Uppsala University, Uppsala, Sweden.
Olschewski, A., Veale, E.L., Nagy, B.M., Nagaraj, C., Kwapiszewska, G., Antigny, F., Lambert, M., Humbert, M., Czirjak, G., Enyedi, P., Mathie, A., 2017. TASK-1 (KCNK3) channels in the lung: from cell biology to clinical implications. Eur. Respir. J. 50, 1700745.
Pisani, D.F., Beranger, G.E., Corinus, A., Giroud, M., Ghandour, R.A., Altirriba, J., Chambard, J.C., Mazure, N.M., Bendahhou, S., Duranton, C., Michiels, J.F., Frontini, A., Rohner-Jeanrenaud, F., Cinti, S., Christian, M., Barhanin, J., Amri, E.Z., 2016. The K+ channel TASK1 modulates beta-adrenergic response in brown adipose tissue through the mineralocorticoid receptor pathway. FASEB J. 30, 909–922.
Qin, C.J., Wen, Z.Y., Wang, J., He, Y., Yuan, D.Y., Li, R., 2018. Uncoupling protein 1 in snakehead (*Channa argus*): Cloning, tissue distribution, and its expression in response to fasting and refeeding. Comp. Biochem. Physiol. A Mol. Integr. Physiol. 225, 1–6.
Roberts, A., 2013. Genetics: Potassium channelopathy implicated in the pathogenesis of familial PAH. Nat. Rev. Cardiol. 10, 550.
Talley, E.M., Bayliss, D.A., 2002. Modulation of TASK-1 (Kcnk3) and TASK-3 (Kcnk9) potassium channels: volatile anesthetics and neurotransmitters share a molecular site of action. J. Biol. Chem. 277, 17733–17742.
Wen, Z.-Y., Xie, B.-W., Qin, C.-J., Wang, J., Yuan, D.-Y., Li, R., Zou, Y.-C., 2017. The complete mitochondrial genome of a threatened loach (*Beaufortia kweichowensis*) and its phylogeny. Conserv. Genet. Resour. 9, 565–568.
Wen, Z.Y., Liang, X.F., He, S., Li, L., Shen, D., Tao, Y.X., 2015. Molecular cloning and tissue expression of uncoupling protein 1, 2 and 3 genes in Chinese perch (*Siniperca chuatsi*). Comp. Biochem. Physiol. B Biochem. Mol. Biol. 185, 24–33.
Xu, J., Bian, C., Chen, K., Liu, G., Jiang, Y., Luo, Q., You, X., Peng, W., Li, J., Huang, Y., Yi, Y., Dong, C., Deng, H., Zhang, S., Zhang, H., Shi, Q., Xu, P., 2017. Draft genome of the Northern snakehead, *Channa argus*. Gigascience 6, 1–5.
Yang, S., Wen, Z.Y., Zou, Y.C., Qin, C.J., Wang, J., Yuan, D.Y., Li, R., 2018. Molecular cloning, tissue distribution, and effect of fasting and refeeding on the expression of neuropeptide Y in *Channa argus*. Gen. Comp. Endocrinol. 259, 147–153.
Zou, Y.-C., Xie, B.-W., Qin, C.-J., Wang, Y.-M., Yuan, D.-Y., Li, R., Wen, Z.-Y., 2017. The complete mitochondrial genome of a threatened loach (*Sinibotia reevesae*) and its phylogeny. Genes & Genomics 39, 767–778.